

On the variability of $I(7620 \text{ \AA})/I(5577 \text{ \AA})$ in low altitude aurora

E. J. Llewellyn¹, R. L. Gattinger¹, A. Vallance Jones²

¹Institute of Space and Atmospheric Studies, Department of Physics and Engineering Physics, 116 Science Place, University of Saskatchewan, Saskatoon, SK S7N 5E2, Canada

E-mail: llewellyn@skisas.usask.ca

²Canadian Space Agency, Ottawa, Canada

Received: 15 June 1998 / Revised: 10 November 1998 / Accepted: 7 December 1998

Abstract. An auroral electron excitation model, combined with simple equilibrium neutral and ion chemistry models, is used to investigate the optical emission processes and height profiles of $I(5577 \text{ \AA})$ and $I(7620 \text{ \AA})$ in the 90 to 100 km altitude region. It is shown that the apparent discrepancies between ground-based and rocket-borne auroral observations of the $I(7620 \text{ \AA})/I(5577 \text{ \AA})$ ratio are due to the extreme height variation of this intensity ratio in the 90 to 100 km region.

Key words. Atmospheric composition and structure (airglow and aurora)

Introduction

Ground-based observations of medium to bright intensity aurora by Gattinger and Vallance Jones (1974) indicate $I(7620 \text{ \AA})/I(5577 \text{ \AA}) \cong 10$, whereas rocket-borne observations by Feldman (1978) report that the ratio is about two. Other rocket-borne observations have suggested the ratio is less than unity (Deans *et al.*, 1976; McDade *et al.*, 1985). As the removal of the airglow component from these rocket observations is straightforward, since the airglow is at a significantly lower altitude than the auroral form as monitored by on-board N_2^+ ING photometers, it is not believed that the reported intensity ratios are contaminated by a large airglow signal. The same is also true for the ground-based observations as the airglow signal is easily removed through subtraction of the measurements in the presence and absence of aurora. In earlier model work for normal aurora, lower border near 110 km, Gattinger *et al.* (1996) obtained intensity ratios for

$I(7620 \text{ \AA})/I(5577 \text{ \AA})$ that were in agreement with the published rocket results and to date the apparent discrepancy between the ground-based and rocket observations has not been explained satisfactorily; although there are some interesting measurements from the ARIES auroral rocket campaign (Vallance Jones *et al.*, 1991). In one case the rocket entered a low altitude aurora, lower border ~ 95 km, and the measurements (Harris, private communication, 1997) suggest that the $I(7620 \text{ \AA})/I(5577 \text{ \AA})$ ratio is probably close to 5. However, it is known that these ARIES measurements were severely contaminated by vehicle-induced glow (Yuen, private communication, 1997) so that the measured intensity ratio cannot be accepted with any confidence. Indeed it is quite possible that vehicle effects could make an in-situ confirmation of the ground-based measurements difficult, if not impossible.

Recent laboratory investigations (Bednaruk *et al.*, 1994) have shown that the 4 eV excited states of O_2 can act as an intermediate and lead to the production of $O_2(b^1\Sigma_g^+)$, the upper state of the oxygen atmospheric band, $I(7620 \text{ \AA})$, in collisions with O_2 or N_2 (reactions 1b and 2b in Table 1). The deactivation of $N_2(A^3\Sigma_u^+)$ molecules by O_2 (reaction 3) is a major source of these excited intermediate states of O_2 (Thomas and Kaufman, 1985). The purpose of the present work is to explain the apparent differences in the measured auroral $I(7620 \text{ \AA})/I(5577 \text{ \AA})$ ratio and it is shown that the inclusion of the $N_2(A^3\Sigma_u^+)$ source of $O_2(b^1\Sigma_g^+)$ results in a significant increase in this ratio when going from 100 km down to 90 km.

Model results and discussion

The electron excitation model used in the present work is the same Monte Carlo implementation that has been described by Gattinger *et al.* (1996). In that work the authors validated the accuracy of their simulation through an extensive comparison of the model results with observations. There have been some recent revisions to the major N_2^+ and O_2^+ electron excitation cross

sections (Doering and Yang, 1997a, b) and these have been incorporated in an updated model. It should be noted that the inclusion of these new reaction rates does not invalidate the earlier work.

In the neutral chemistry computations, the branching ratios for O₂ and N₂ in reactions 1b and 2b that were determined by Bednaruk *et al.* (1994) have both been scaled by 0.4 to agree with more recent measurements (Copeland, private communication, 1997). The model results for height profiles of volume production rates, optical emission rates, and emission rate ratios for the relevant species are discussed in the following sections. The background atmosphere, including [O], is taken from MSIS (Hedin, 1987) for the mid-winter auroral zone under moderate solar activity conditions. Additional model results with [O] scaled by 0.5 are also included to demonstrate the sensitivity of the ratios to [O] variations.

The assumed precipitating electron energy spectrum is a 50 keV monoenergetic beam isotropic in the downward direction. The theoretical emission ratio results for a Maxwellian distribution with a characteristic energy of 25 keV are also included in order to demonstrate the sensitivity of the ratios to the assumed electron spectrum.

The volume production and emission rates are arbitrarily normalized to an input flux of 1 erg cm⁻²s⁻¹. The energy flux in low altitude aurora tends to be considerably greater, but, except for induced composition changes, the atmospheric response to precipitating electrons is approximately linear.

In the 95 km region [NO] changes can be induced by high energy and high flux electron precipitation (Swider and Narcisi, 1977). Among the ion chemistry processes (Vallance Jones, 1974) the dissociative recombination rate of O₂⁺ is a major contributor to the production rate of O(¹S) and O(¹D) and hence, according to reaction 4, O₂(b¹Σ_g⁺). As [NO] has a significant impact on [O₂⁺], the effect of [NO] variations is also included; model estimates are included for [NO] set to both [O]/1000 and to [O]/100 in agreement with normal [NO] and high [NO] conditions.

O(¹S) production

As shown in Fig. 1a the major O(¹S) source in the 100 km region is through reaction 5, the energy transfer

from N₂(A³Σ_u⁺). Minor sources include O₂⁺ dissociative recombination (branching ratio 0.1), direct electron excitation of O, and energy transfer from O₂^{*} (reaction 6) where O₂^{*} is formed through reaction 3 plus a minor contribution from the 6 eV electron energy loss feature (Gattinger *et al.*, 1996). At 90 km the major source of O(¹S) is from O₂⁺ dissociative recombination. The volume emission rate (VER) of the 5577 Å emission is also included in Fig. 1a. It is reduced from the O(¹S) production rate profile by the component branching to the 2972 Å emission and through quenching by O₂.

For the high [NO] case (Fig. 1b) the O₂⁺ dissociative recombination source is reduced by nearly an order of magnitude and the N₂(A³Σ_u⁺) energy transfer mechanism remains dominant to below 90 km.

O(¹D) production

The major O(¹D) source in the 100 km region (Fig. 2a) is from dissociative excitation in the Schumann-Runge continuum; Itikawa *et al.* (1989) have summarized the relevant O₂ cross sections. Other important sources include direct electron excitation of O, cascading from O(¹S), and O₂⁺ dissociative recombination (branching ratio 1.0). At 90 km the major source of O(¹D) is from O₂⁺ dissociative recombination. In the 100 km altitude region the O(¹D) state is completely quenched by N₂ and O₂ although approximately 15% reappears via energy transfer in the O₂(b¹Σ_g⁺) state.

For the high [NO] case (Fig. 2b) the O₂⁺ dissociative recombination source is scaled down by nearly an order of magnitude resulting in the O₂ Schumann-Runge source becoming dominant to altitudes below 90 km.

O₂(b¹Σ_g⁺) production

As shown in Fig. 3a the major O₂(b¹Σ_g⁺) source in the 100 km region is energy transfer from O(¹D) (reaction 4). Other important sources include energy transfer from N₂(A³Σ_u⁺) (reaction 3 followed by reactions 1b and 2b), and by direct electron impact excitation of O₂. Energy transfer from O₂^{*} (produced by the 6 eV feature) through reactions 1b and 2b is also included as a source of O₂(b¹Σ_g⁺) molecules. At 90 km the N₂(A³Σ_u⁺) energy transfer mechanism is the dominant source of O₂(b¹Σ_g⁺). The O₂(b¹Σ_g⁺) state is quenched by N₂ at altitudes below

Table 1. Reaction rates used in the model, units are cm³ molecule s⁻¹

O ₂ [*] + O ₂	→	O ₂ ^{**} , O ₂ + O ₂	2.8 × 10 ⁻¹¹	Bednaruk <i>et al.</i> (1994)	1a
	→	O ₂ (b ¹ Σ _g ⁺) + O ₂	2.8 × 10 ⁻¹²	See text	1b
O ₂ [*] + N ₂	→	O ₂ ^{**} , O ₂ + N ₂	1.4 × 10 ⁻¹¹	Bednaruk <i>et al.</i> (1994)	2a
	→	O ₂ (b ¹ Σ _g ⁺) + N ₂	3.0 × 10 ⁻¹²	See text	2b
N ₂ (A ³ Σ) + O ₂	→	O ₂ [*] + N ₂	4.2 × 10 ⁻¹² (T/300) ^{0.55}	Gattinger <i>et al.</i> (1996)	3
O(¹ D) + O ₂	→	O ₂ (b ¹ Σ _g ⁺) + O ₂	1.7 × 10 ⁻¹¹ e ^{67.5/T}	Snelling and Gauthier (1971)	4
N ₂ (A ³ Σ) + O	→	O(¹ S) + N ₂	8.2 × 10 ⁻¹²	Gattinger <i>et al.</i> (1996)	5
O ₂ ⁺ + O	→	O(¹ S) + O ₂	2.6 × 10 ⁻¹¹	Gattinger <i>et al.</i> (1996)	6
NO + O ₂ ⁺	→	NO ⁺ + O ₂	8.0 × 10 ⁻¹⁰	Vallance Jones (1974)	7

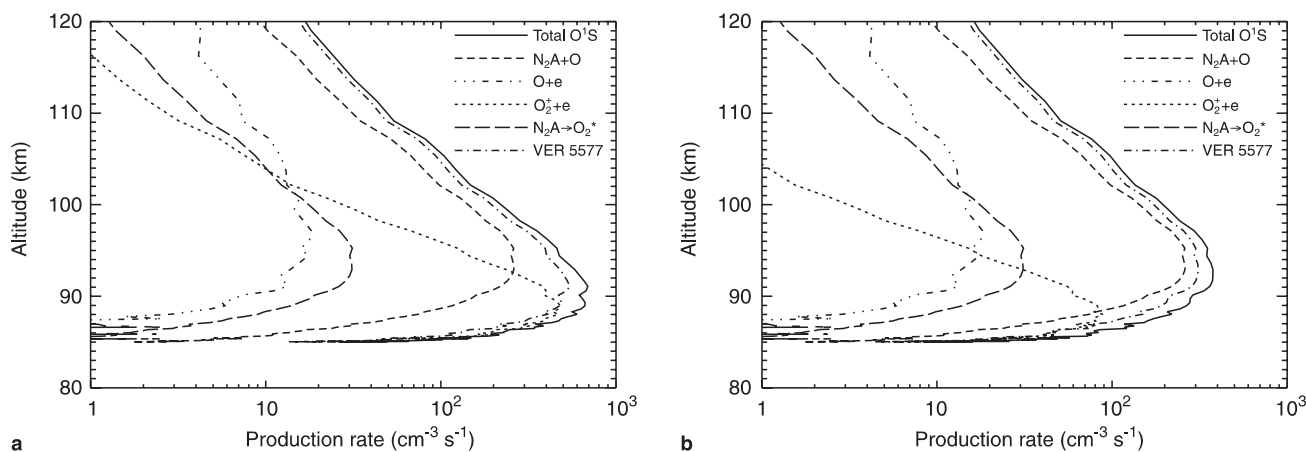


Fig. 1. **a** O^1S production rates from various sources with normal [NO] and a 50 keV monoenergetic electron spectrum. The resultant volume emission rate (VER) of 5577 Å is shown. **b** Same as **a** but with high [NO]

approximately 100 km and emits in both the 0-0 band at 7620 Å and the 0-1 band at 8645 Å; the resultant volume emission rate (VER) of the 7620 Å emission is included in Fig. 3a.

For the high [NO] case (Fig. 3b) the $N_2(A^3\Sigma_u^+)$ energy transfer mechanism is the dominant $O_2(b^1\Sigma_g^+)$ source throughout the 90 to 100 km region; the O^1D energy transfer source is reduced by a factor of about two in the 90 km region.

Emission rates relative to $I(3914 \text{ \AA})$

The calculated optical emission rates, relative to $I(3914 \text{ \AA})$, are shown Fig. 4a for monoenergetic 50 keV electrons under normal [NO] conditions. The $I(7620 \text{ \AA})/I(3914 \text{ \AA})$ ratio at 90 km is approximately equal to the 110 km value while the $I(5577 \text{ \AA})/I(3914 \text{ \AA})$ ratio at 90 km is about 1/3 the 110 km value. The calculated model $I(O_2^+ 1NG)/I(3914 \text{ \AA})$ ratio at 90 km is about 50% higher than at 110 km, this is in agreement with the observations of Type-B aurora reported by Evans and Vallance Jones (1965).

For the high [NO] case (Fig. 4b) the $I(7620 \text{ \AA})/I(3914 \text{ \AA})$ ratio at 90 km is approximately 50% smaller than the 110 km value while the $I(5577 \text{ \AA})/I(3914 \text{ \AA})$ ratio at 90 km is nearly an order of magnitude lower than the 110 km value.

The emission ratios for an assumed Maxwellian electron energy spectrum with a characteristic energy of 25 keV and for normal [NO] are shown in Fig. 4c. As expected the results are nearly identical with those of Fig. 4a and clearly indicate that the emission intensity ratios are primarily dependent on the emission altitude. Thus a low $I(7620 \text{ \AA})/I(3914 \text{ \AA})$ ratio requires energetic electron precipitation that can reach the 90–95 km altitude region.

The $I(7620 \text{ \AA})/I(5577 \text{ \AA})$ ratio

The $I(7620 \text{ \AA})/I(5577 \text{ \AA})$ ratios for both normal and high [NO] cases are plotted in Fig. 5. The ratio variations with MSIS [O] and MSIS [O]/2 have also been modelled to cover the [O] range determined by

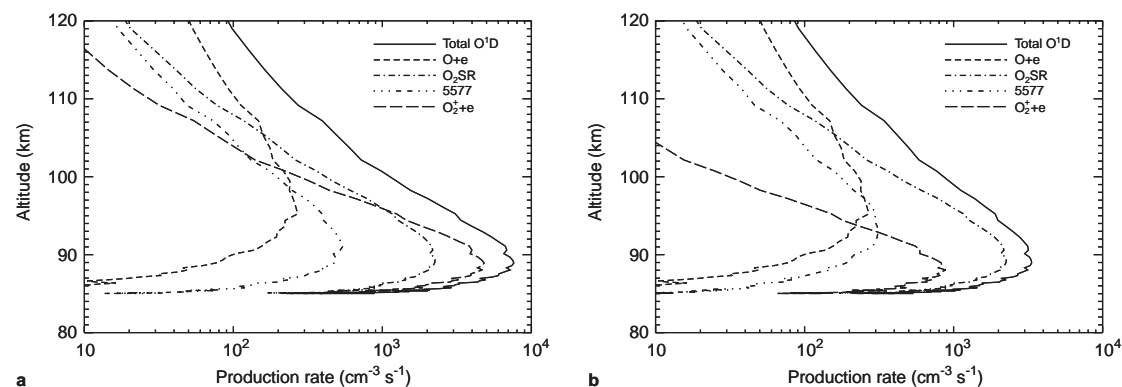


Fig. 2. **a** O^1D production rates from various sources with normal [NO] and a 50 keV monoenergetic electron spectrum. The O^1D state is completely quenched in the 100 km region. **b** Same as **a** but with high [NO]

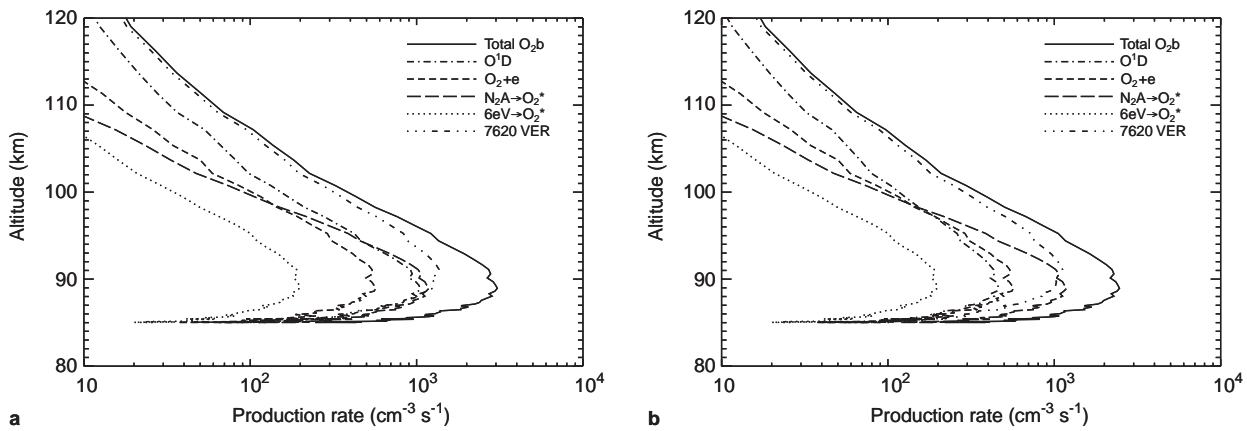


Fig. 3. **a** $O_2(b^1\Sigma_g^+)$ production rates from various sources with normal $[NO]$ and a 50 keV monoenergetic electron spectrum. The resultant 7620 Å volume emission rate (VER) is also given. **b** Same as **a** but with high $[NO]$

Gattinger *et al.* (1996). For the enhanced $[NO]$ cases the $I(7620 \text{ \AA})/I(5577 \text{ \AA})$ ratio increases by approximately three to five times in going from 110 km down to 90 km; for the normal $[NO]$ the ratio increase is much smaller. In order to compare these calculated volume emission rates with in-situ rocket observations it is important to note the rocket observations of $I(7620 \text{ \AA})/I(5577 \text{ \AA})$ are referred to the zenith. According to Fig. 5, a variation by a factor of up to two in

this ratio *would be expected* if the peak emission altitudes between flights varied by about 10 km in the 105 km altitude region.

Unlike the rocket-borne observations the ground-based observations of Gattinger and Vallance Jones (1974) were not made in the zenith, but rather at much lower elevation angles. Thus, the spectra are weighted towards the bright lower borders of the auroral forms. The lower borders for bright aurora are frequently well

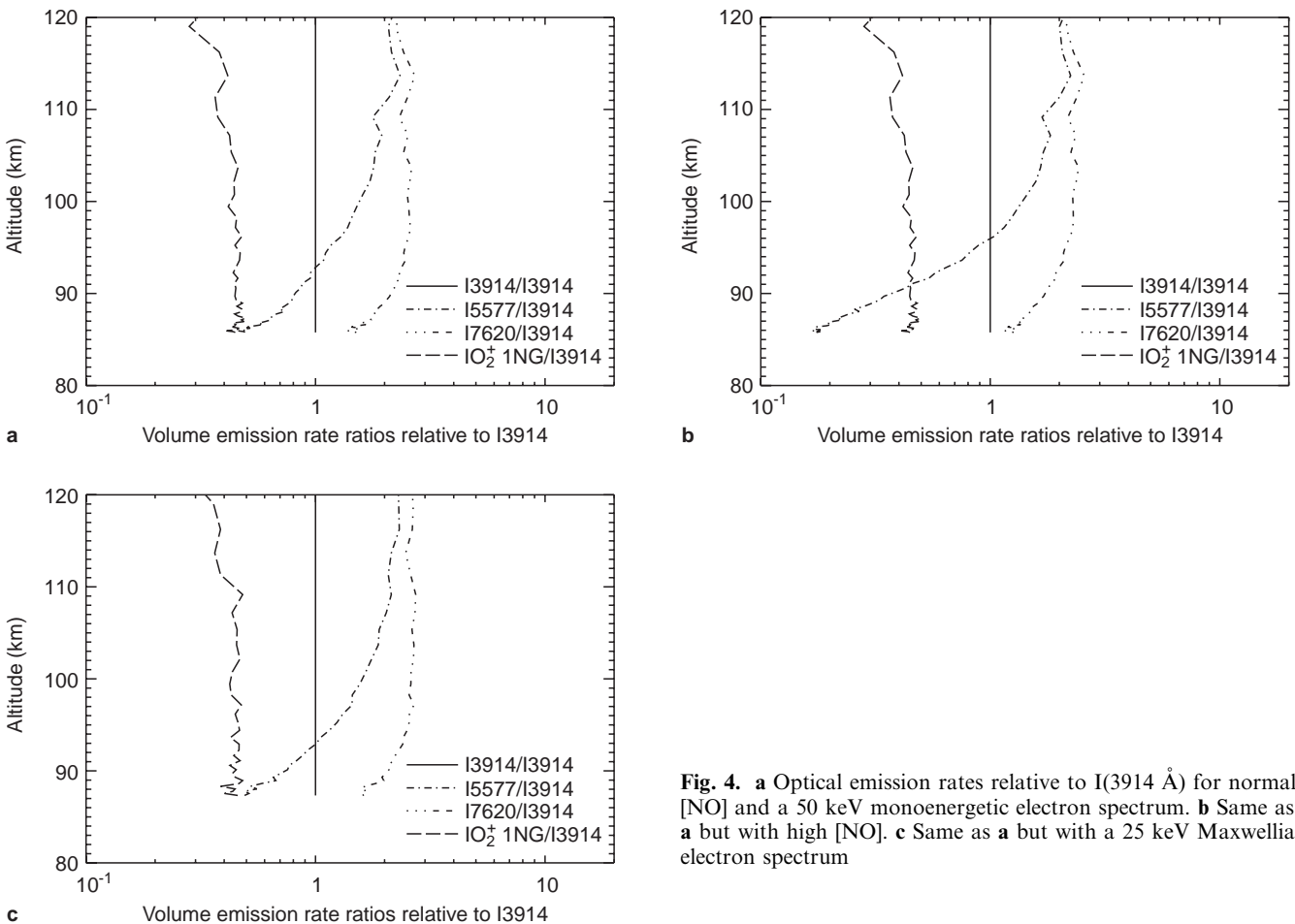


Fig. 4. **a** Optical emission rates relative to $I(3914 \text{ \AA})$ for normal $[NO]$ and a 50 keV monoenergetic electron spectrum. **b** Same as **a** but with high $[NO]$. **c** Same as **a** but with a 25 keV Maxwellian electron spectrum

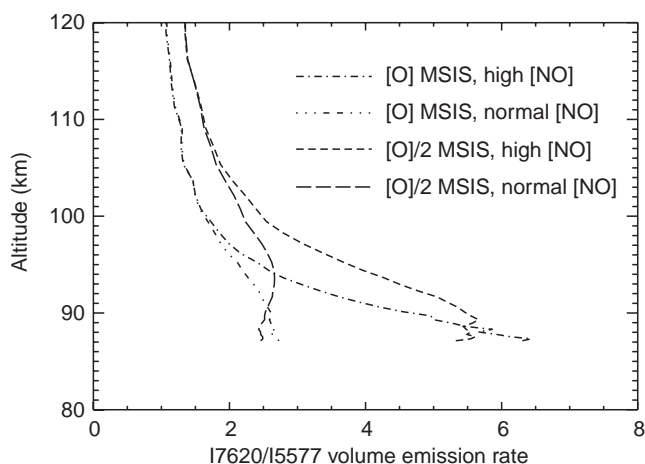


Fig. 5. Modelled $(7620 \text{ \AA})/(5577 \text{ \AA})$ emission ratios for normal and high [NO], 50 keV monoenergetic electron spectrum, and for MSIS [O] and MSIS [O]/2

below 100 km. It is important to note the lower borders do not exhibit the characteristic pink Type-B colour until the height decreases to about 90 km (Gattinger *et al.*, 1985). According to Fig. 5, $I(7620 \text{ \AA})/I(5577 \text{ \AA}) \cong 4$ in the 95 km region, and can increase to more than 5 at 90 km in some cases. This is consistent with the ground-based results reported by Gattinger and Vallance Jones (1974), although the modelled ratio does not reach the measured value of 10. Unfortunately, it is extremely difficult to make ground-based observations of the oxygen atmospheric band in normal aurora so that direct confirmation of the rocket observations cannot be made with any confidence. The reason for this is that ground-based observations of the atmospheric band must be made with the weaker (factor 17) 0-1 band at 8645 \AA as the 0-0 band at 7620 \AA is fully absorbed by the underlying atmospheric column. Hence, unless the aurora is particularly bright, which usually means a lower emission altitude, it is very difficult to make reliable ground-based measurements of the $I(7620 \text{ \AA})/I(5577 \text{ \AA})$ ratio.

Conclusions

Clearly, from the results of our model calculations, there is no contradiction in the reported $I(7620 \text{ \AA})/I(5577 \text{ \AA})$ auroral intensity ratios for ground-based and in-situ rocket observations. These apparent differences can be directly attributed to the strong variation of the $I(7620 \text{ \AA})/I(5577 \text{ \AA})$ ratio with altitude. In the 100 km to 120 km region the ratio can vary up to a factor of three. In the 90 km region the ratio can reach a factor of six. The model calculations also indicate that enhanced [NO] is an important contributor to the ground based measurements of the $I(7620 \text{ \AA})/I(5577 \text{ \AA})$ ratio. The difference between the model ratio values and the reported observational value of 10 suggests that the efficiency, and the rate constant, for other vibrational levels (reactions 1b, 2b and 3) may be different from those adopted in the present work. This is, of course,

consistent with the apparent uncertainties for the reported vibrational dependence of the yield of $O(^1S)$ in the energy transfer from $N_2(A^3\Sigma_u^+)$ that has been discussed by Gattinger *et al.* (1996). However, it is also possible that the observed intensity ratios may have been influenced by rapid temporal and spatial changes of the aurora within the observed field-of-view, thus the agreement between the model and observations may be better than is apparent. The strong variation of the $I(7620 \text{ \AA})/I(5577 \text{ \AA})$ ratio with altitude in the aurora mimics the altitude variation of this intensity ratio in the airglow and so provides indirect evidence that both the auroral and the airglow excitation mechanisms (McDade *et al.*, 1986) involve energy transfer, although the initiating excited state is apparently different in the two cases. The direct confirmation of the present calculations with conventional rocket sounding is extremely difficult; low altitude aurora is normally active and, as noted previously, direct measurements are also complicated by the presence of rocket glow (Murtagh *et al.*, 1997). However, it is possible that tomographic observations of the type described by McDade and Llewellyn (1991) could provide confirmation of the model calculations.

Acknowledgements. The authors wish to express their sincere thanks to an anonymous referee for the very careful review and valuable comments. This work has been supported through Grants-in-Aid from the Natural Sciences and Engineering Research Council of Canada.

Topical Editor F. Vial thanks G. R. Swenson and G. J. Romick for their help in evaluating this paper.

References

- Bednaruk, G., R. P. Wayne, J. Wildt, and E. H. Fink, The yield of $O_2(b^1\Sigma_g^+, v=0)$ produced by quenching of $O_2(A^3\Sigma_u^+, v=8)$ by O_2 , *Chem. Phys.*, **185**, 251, 1994.
- Deans, A. J., G. G. Shepherd, and W. F. J. Evans, A rocket measurement of the $O_2(b^1\Sigma_g^+ - X^3\Sigma_g^-)(0-0)$ atmospheric band in aurora, *J. Geophys. Res.*, **81**, 6227, 1976.
- Doering, J. P., and J. Yang, Direct experimental measurement of electron impact ionization-excitation branching ratios: 3. Branching ratios and cross sections for the $N_2^+ X^2\Sigma_u^+, A^2\Pi_u$, and $B^2\Sigma_u^+$ states at 100 eV, *J. Geophys. Res.*, **102**, 9683, 1997a.
- Doering, J. P., and J. Yang, Direct experimental measurement of electron impact ionization-excitation branching ratios: 4. Branching ratios and cross sections for O_2^+ at 100 eV, *J. Geophys. Res.*, **102**, 9691, 1997b.
- Evans, W. F. J., and A. Vallance Jones, Some observations of Type-B red aurora with a multichannel photometer, *Can. J. Phys.*, **43**, 697, 1965.
- Feldman, P. D., Auroral excitation of optical emissions of atomic and molecular oxygen, *J. Geophys. Res.*, **83**, 2511, 1978.
- Gattinger, R. L., and A. Vallance Jones, Quantitative spectroscopy of the aurora. II. The spectrum of medium intensity aurora between 4500 and 8900 Å, *Can. J. Phys.*, **52**, 2343, 1974.
- Gattinger, R. L., F. R. Harris, and A. Vallance Jones, The height, spectrum and mechanism of Type-B red aurora and its bearing on the excitation of $O(^1S)$ in aurora, *Planet. Space Sci.*, **33**, 207, 1985.
- Gattinger, R. L., E. J. Llewellyn, and A. Vallance Jones, On $I(5577 \text{ \AA})$ and $I(7620 \text{ \AA})$ auroral emissions and atomic oxygen densities, *Ann. Geophysicae*, **14**, 687, 1996.
- Hedin, A. E., MSIS-86 thermospheric model, *J. Geophys. Res.*, **92**, 4649, 1987.

- Itikawa, Y., A. Ichimura, K. Onda, K. Sakimoto, K. Takayanagi, Y. Hatano, M. Hayashi, H. Nishimura, and S. Tsurubuchi**, Cross sections for collisions of electrons and photons with oxygen molecules, *J. Phys. Chem. Ref. Data*, **18**, 23, 1989.
- McDade, I. C., and E. J. Llewellyn**, Inversion techniques for recovering two-dimensional distributions of auroral emission rates from tomographic rocket photometer measurements, *Can. J. Phys.*, **69**, 1059, 1991.
- McDade, I. C., E. J. Llewellyn, and F. R. Harris**, A rocket measurement of the $O_2(b^1\Sigma_g^+ - X^3\Sigma_g^-)(0-0)$ Atmospheric band in a pulsating aurora, *Can. J. Phys.*, **63**, 1322, 1985.
- McDade, I. C., D. P. Murtagh, R. G. H. Greer, P. H. G. Dickinson, G. Witt, J. Stegman, E. J. Llewellyn, L. Thomas, and D. B. Jenkins**, ETON 2: quenching parameters for proposed precursors of $O_2(b^1\Sigma_g^+)$ and $O(^1S)$ in the terrestrial nightglow, *Planet. Space Sci.* **34**, 789–800, 1986.
- Murtagh, D. P., E. J. Llewellyn, and P. J. Espy**, Infra-red rocket glow: A mechanistic analysis, *Geophys. Res. Letts*, **24**, 85, 1997.
- Snelling, D. R., and M. Gauthier**, Efficiency of $O_2(^1\Sigma_g^+)$ formation by $O(^1D) + O_2$, *Chem. Phys. Lett.*, **9**, 254, 1971.
- Swider, W., and R. S. Narcisi**, Auroral E-region: ion composition and nitric oxide, *Planet. Space Sci.*, **25**, 103, 1977.
- Thomas, J. M., and F. Kaufman**, Rate constants of the reactions of metastable $N_2(A^3\Sigma_u^+)$ in $v = 0, 1, 2,$ and 3 with ground state O_2 and O , *J. Chem. Phys.*, **83**, 2900, 1985.
- Vallance Jones, A.**, *Aurora*, Reidel, Dordrecht, 1974.
- Vallance Jones, A., R. L. Gattinger, F. Creutzberg, F. R. Harris, A. G. McNamara, A. W. Yau, E. J. Llewellyn, D. Lummerzheim, M. H. Rees, I. C. McDade, and J. Margot-Chaker**, Characterization and modelling of an evening auroral arc observed from a rocket and a ground-based line of meridian scanners, *Planet. Space Sci.*, **39**, 1677, 1991.